$Na_2[VB_3P_2O_{12}(OH)]\cdot 2.92H_2O$: A New Open-Framework Vanadium Borophosphate Containing Extra-Large 16-Ring Pore Openings and $12^8 16^6$ Super Cavities Synthesized by Using the Boric Acid Flux Method

Weiting Yang, Jiyang Li, Qinhe Pan, Zhao Jin, Jihong Yu,* and Ruren Xu

State Key Laboratory of Inorgnic Synthesis and Preparative Chemistry, College of Chemistry, Jinlin University, Changchun 130012, P.R. China

Received January 4, 2008. Revised Manuscript Received May 5, 2008

A new three-dimensional (3-D) open-framework vanadium (IV) borophosphate, $Na_2[VB_3P_2O_{12}(OH)]\cdot 2.92H_2O$ (denoted as VBPO-CJ27), has been synthesized by using boric acid flux method. Single-crystal structure analysis reveals that its structure is constructed by the connection of VO_6 octahedra, PO_4 and BO_4 tetrahedra, and $BO_2(OH)$ trigonal planes to form a 3-D anionic framework containing intersecting 8-, 12-, and 16-ring channels. Charge neutrality is achieved by Na^+ ions, and the guest water molecules locate in the void space of the open framework. To the best of our knowledge, it is the first borophosphate with extra-large 16-ring openings. Interestingly, its structure features unprecedented $12^8 16^6$ super cavities. The compound is further characterized by SEM, powder XRD, ICP, TGA, and IR analyses. Its magnetic property and ion-exchange capacity are also studied. The magnetic measurement reveals that VBPO-CJ27 is paramagnetic. Ion-exchange studies show that Na^+ ions can be partially exchanged by NH_4^+ ions.

Introduction

Borophosphates have been widely studied for their fascinating structural architectures and potential applications in optical, magnetic, and catalytic aspects.[1–6] Since the first zeolite-like metal borophosphate $(C_2H_{10}N_2)[CoB_3P_3O_{12}(OH)_{12}]$[7] was discovered in 1996, a large number of open-framework borophosphates have been prepared under hydrothermal conditions.[8–10] Alternatively, boric acid flux method has been used for the syntheses of boron-containing open-framework compounds, such as aluminoborates, rare earth polyborates, and other borates,[11] as well as borophosphates $NH_4[BPO_4F]$ (GIS)[12] and $(NH_4)_{16}[Zn_{16}B_8P_{24}O_{96}]$ (ANA)[13] with known zeotype structures. In this method, boric acid melts at 175 °C, and excessive melting boric acid acts as both the reaction medium and the reactant. Notably, the employment of the boric acid flux method has produced several open frameworks with extra-large pore openings, such as aluminoborate PKU-1[11a] with 18-ring channels and $MCuB_7O_{12}\cdot nH_2O$ (M = Na, K)[14] with 14-ring channels. The exploration of new extra-large microporous open-framework borophosphates by using this method has aroused great interest.

The borophosphate frameworks are featured by various anionic partial structures, such as oligomeric units, one-dimensional (1-D) chains and ribbons, two-dimensional (2-D) layers, and three-dimensional (3-D) open frameworks.[3,15] Among them, only a few structures, including $NH_4[BPO_4F]$,[12] $M[B_2P_2O_8(OH)]$ (M = Rb, Cs),[16] and M^IBeBPO ($M^I = K^+$, Na^+, and NH_4^+)[17] possess 3-D anionic partial structures. Another structural feature of borophosphates is that the B atom commonly adopts tetrahedral coordination and that the B/P ratios are usually equal to or less than 1.0. Only a few borophosphates, containing both BO_3 and BO_4 coordinations, have a B/P ratio higher than

* Corresponding author. E-mail: jihong@jlu.edu.cn.

(1) Cheetham, A. K.; Férey, G.; Loiseau, T. *Angew. Chem., Int. Ed.* **1999**, *38*, 3268.
(2) Pan, S. L.; Wu, Y. C.; Fu, P. Z.; Zhang, G. C.; Li, Z. H.; Du, C. X.; Chen, C. T. *Chem. Mater.* **2003**, *15*, 2218.
(3) Ewald, B.; Huang, Y. X.; Kniep, R. *Z. Anorg. Allg. Chem.* **2007**, *633*, 1517, and references therein.
(4) Yang, M.; Yu, J. H.; Shi, L.; Chen, P.; Li, G. H.; Chen, Y.; Xu, R. R. *Chem. Mater.* **2006**, *18*, 476.
(5) Ahmed, K.; Geisert, C. *J. Vac. Sci. Technol., A* **1992**, *10*, 313.
(6) Kniep, R.; Gözel, G.; Eisenmann, B.; Röhr, C.; Asbrand, M.; Kizilyalli, M. *Angew. Chem., Int. Ed. Engl.* **1994**, *33*, 749.
(7) Sevov, S. C. *Angew. Chem., Int. Ed. Engl.* **1996**, *35*, 2630.
(8) Kniep, R.; Will, H. G.; Boy, I.; Röhr, C. *Angew. Chem., Int. Ed. Engl.* **1997**, *36*, 1013.
(9) Kniep, R.; Schäfer, G.; Engelhardt, H.; Boy, I. *Angew. Chem., Int. Ed.* **1999**, *38*, 3642.
(10) Hang, Y. X.; Schäfer, G.; Carrillo-Cabrera, W.; Borrmann, H.; Gil, R. C.; Kniep, R. *Chem. Mater.* **2003**, *15*, 4930.
(11) (a) Ju, J.; Lin, J. H.; Li, G. B.; Yang, T.; Li, H. M.; Liao, F. H.; Loong, C.-K.; You, L. P. *Angew. Chem., Int. Ed.* **2003**, *425*, 607. (b) Lu, P. C.; Wang, Y. X.; Lin, J. H.; You, L. P. *Chem. Commun.* **2001**, 1178. (c) Williams, I. D.; Wu, M. M.; Sung, H. H-Y.; Zhang, X. X.; Yu, J. H. *Chem. Commun* **1998**, 2634.
(12) Li, M. R.; Liu, W.; Ge, M. H.; Chen, H. H.; Yang, X. X.; Zhao, J. T. *Chem. Commun.* **2004**, 1272.
(13) Yang, M.; Yu, J. H.; Chen, P.; Li, J. Y.; Fang, Q. R.; Xu, R. R. *Microporous Mesoporous Mater.* **2005**, *87*, 124.
(14) Yang, T.; Li, G. B.; You, L. P.; Ju, J.; Liao, F. H.; Lin, J. H. *Chem. Commun.* **2005**, 4225.
(15) Kniep, R.; Engelhardt, H.; Hauf, C. *Chem. Mater.* **1998**, *10*, 2930, and references therein.
(16) Hauf, C.; Kniep, R. *Z. Naturforsch.* **1997**, *52b*, 1432.
(17) Zhang, H. Y.; Chen, Z. X.; Weng, L. H.; Zhou, Y. M.; Zhao, D. Y. *Microporous Mesoporous Mater.* **2003**, *57*, 309.

10.1021/cm8000283 CCC: $40.75
Published on Web 07/01/2008

1.0.[18,19] Up to date, the largest pore opening in known borophosphate materials is limited to 12-rings. Notable examples are known as $(C_4N_3H_{16})[Zn_3B_3P_6O_{24}]\cdot H_2O$[20] and MBPO-CJ25 (M = Mn, Co, Ni).[19a] The synthesis of extra-large microporous open-framework borophosphates is of great challenge.

Herein we report the first open-framework vanadium borophosphate $Na_2[VB_3P_2O_{12}(OH)]\cdot 2.92H_2O$ (denoted as VBPO-CJ27) with extra-large 16-ring channels. It contains intersecting 8-, 12-, and 16-ring channels and unprecedented $12^8 16^6$ supercavities synthesized by the boric acid flux method. Its magnetic property and ion-exchange capacity have been investigated.

Experimental Section

Synthesis. The title compound was prepared by a boric acid flux method in the reaction system with molar compositions of 16.2 H_3BO_3:1.0 V_2O_5:(1.0−1.4) $Na_2HPO_4\cdot 12H_2O$. Typically, a mixture of 1 g of H_3BO_3, 0.182 g of V_2O_5, and 0.5 g of $Na_2HPO_4\cdot 12H_2O$ was directly added into a 15 mL Teflon lined stainless steel autoclave and heated at 200 °C for 5 days. The final product containing large bright blue single crystals in the form of dodecahedron was washed with hot water (50 °C) until the residual H_3BO_3 was completely removed and then dried in air.

Characterization. The scanning electron microscopy(SEM) image was taken on a JSM-6700F electron microscope operating at 5.0 kV. X-ray powder diffraction (XRD) data were collected on a Siemens D5005 diffractometer with Cu Kα radiation ($\lambda = 1.5418$ Å). Inductively coupled plasma (ICP) analysis was performed on a Perkin-Elmer Optima 3300Dv spectrometer. Thermogravimetric analysis (TGA) was carried out on a NETZSCH STA 449C TG/DTA analyzer in N_2 with a heating rate of 10 °C/min. The infrared (IR) spectrum was recorded within the 400−4000 cm^{-1} region on a Bruker-IFS 66V/S spectrometer using KBr pellets. Temperature-dependent magnetic susceptibility data were recorded on a Quantum-Design MPMS-XL SQUID magnetometer under an applied field of 5 kOe over the temperature range of 4−300 K.

Single-Crystal Structure Determination. A suitable single crystal was selected for single-crystal X-ray diffraction analysis. The data were collected on a Siemens SMART CCD diffractometer using graphite-monochromated Mo Kα radiation ($\lambda = 0.71073$ Å) at a temperature of 20 ± 2 °C. Data processing was accomplished with the SAINT processing program.[21] The structure was solved by direct method and refined by full matrix least-squares technique with the SHELXTL crystallographic software package.[22] The V, B, P, and O atoms of the framework could be unambiguously located. The Na^+ ions and Ow atoms were subsequently located from a difference Fourier map whose fractional occupancies were determined according to the charge balance as well as the compositional and TG analyses. The H atoms associated with the hydroxyl of the $BO_2(OH)$ groups were added theoretically. Experimental details for crystal determination are listed in Table 1.

Table 1. Crystal Data and Structure Refinement for VBPO-CJ27[a]

compound	VBPO-CJ27
empirical formula	$H_{3.42}B_{1.50}NaO_{7.96}PV_{0.50}$
formula weight	226.42
temperature	293(2) K
wavelength	0.71073 Å
crystal system, space group	cubic, $I\bar{4}3m$
unit cell dimensions	$a = 20.1007(7)$ Å
volume	8121.4(5) Å^3
Z, calculated density	48, 2.222 Mg/m^3
absorption coefficient	1.121 mm^{-1}
$F(000)$	5380
theta range for data collection	1.43 to 28.28°
limiting indices	$-26 \le h \le 26$, $-25 \le k \le 26$, $-15 \le l \le 26$
reflections collected/unique	25800/1845 [R(int) = 0.0693]
completeness to θ	28.28°, 98.6%
refinement method	Full-matrix least-squares on F^2
data/restraints/parameters	1845/0/126
goodness-of-fit on F^2	1.056
final R indices [$I > 2\sigma(I)$]	$R_1 = 0.0728$, $wR_2 = 0.2165$
R indices (all data)	$R_1 = 0.0830$, $wR_2 = 0.2287$
largest diff. peak and hole	1.088 and −1.901 e Å^{-3}

[a] $R_1 = \sum(\Delta F/\sum(F_o))$; $wR_2 = (\sum[w(F_o^2 - F_c^2)])/\sum[w(F_o^2)^2]^{1/2}$, $w = 1/\sigma^2(F_o^2)$.

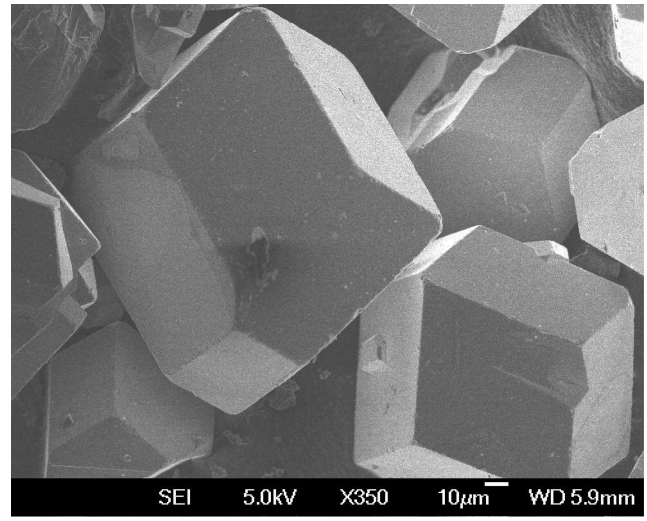

Figure 1. SEM image of VBPO-CJ27.

Results and Discussion

Synthesis and Characterization. VBPO-CJ27 was prepared in the reaction system of $H_3BO_3-V_2O_5-Na_2HPO_4\cdot 12H_2O$ at 200 °C for 5 days. In the reaction, the amount of boric acid was excessive, and a little amount of water decomposed from H_3BO_3 and $Na_2HPO_4\cdot 12H_2O$ was necessary. The compound could also be synthesized by using $NaH_2PO_4\cdot 2H_2O$ and NH_4VO_3 as phosphorus and vanadium sources, respectively, under similar conditions.

Figure 1 shows the scanning electron microscope image of the as-synthesized VBPO-CJ27 product, and large single crystals in the form of dodecahedron can be clearly observed. Figure 2 shows the powder XRD pattern of VBPO-CJ27, which is in agreement with the simulated one generated on the basis of single-crystal structural data, proving the phase purity of the as-synthesized product. Inductively coupled

(18) (a) Boy, I.; Kniep, R. *Z. Naturforsch.* **1999**, *54b*, 895. (b) Hauf, C.; Kniep, R. *Z. Kristallogr.* **1996**, *211*, 705. (c) Hauf, C.; Kniep, R. *Z. Kristallogr.* **1996**, *211*, 707. (d) Hauf, C.; Kniep, R. *Z. Kristallogr.* **1997**, *212*, 313. (e) Xiong, D. B.; Chen, H. H.; Yang, X. X.; Zhao, J. T. *J. Solid State Chem.* **2007**, *180*, 232.

(19) (a) Yang, M.; Yu, J. H.; Di, J. C.; Li, J. Y.; Chen, P.; Fang, Q. R.; Chen, Y.; Xu, R. R. *Inorg. Chem.* **2006**, *45*, 3588. (b) Yang, T.; Li, G. B.; Ju, J.; Liao, F. H.; Xiong, M.; Lin, J. H. *J. Solid State Chem.* **2006**, *179*, 2513. (c) Liu, W.; Huang, Y. X.; Cardoso, R.; Schnelle, W.; Kniep, R. *Z. Anorg. Allg. Chem.* **2006**, *632*, 2143.

(20) Liu, W.; Li, M. R.; Chen, H. H.; Yang, X. X.; Zhao, J. T. *Dalton Trans.* **2004**, 2847.

(21) *SMART and SAINT* (software packages); Siemens Analytical X-ray Instruments, Inc.: Madison, WI, 1996.

(22) *SHELXTL Program*, version 5.1; Siemens Industrial Automation, Inc.: Madison, WI, 1997.

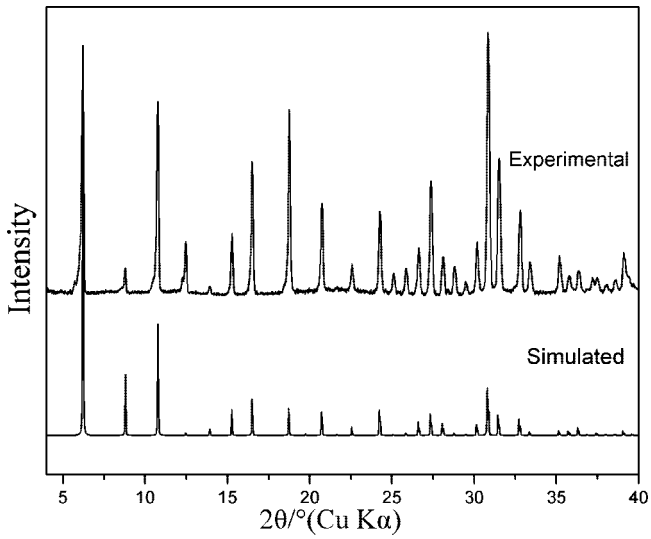

Figure 2. Simulated and experimental powder X-ray diffraction patterns of VBPO-CJ27.

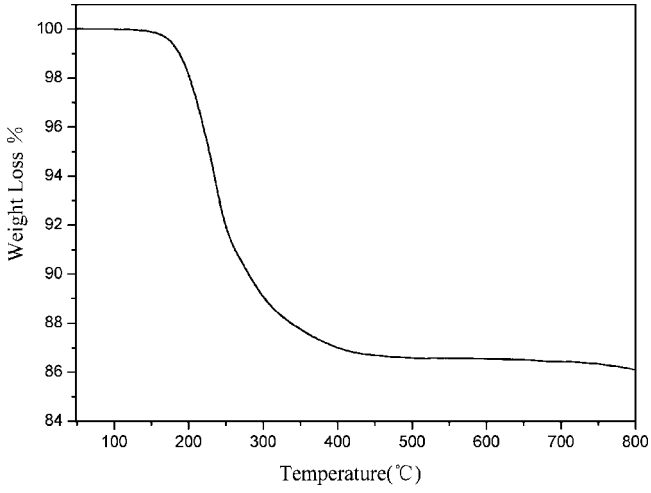

Figure 3. TG curve of VBPO-CJ27.

plasma (ICP) analysis gave the contents of V, B, P, and Na as 10.66, 7.90, 14.20 and 10.64 wt %, which are in agreement with the calculated values of 11.25, 7.16, 13.68, and 10.15 wt %, respectively, based on the formula given by single-crystal structure analysis. The TGA curve shows a major weight loss of 13.9 wt % occurring at 185−410 °C (Figure 3), which is ascribed to the removal of the guest H_2O molecules and OH groups (calcd 13.59 wt %) in the product. The XRD studies show that the compound is stable at 350 °C upon calcination and collapses at 400 °C. Figure 4 shows the IR spectrum of VBPO-CJ27. The bands at 3456 and 1641 cm^{-1} can be assigned to the stretching and bending vibrations of O−H groups and H_2O molecules, while the bands at 1433 and 1217 cm^{-1} correspond to the stretching and bending vibrations of BO_3 groups. The bands in the region 1101−549 cm^{-1} can be assigned to the asymmetric stretching and bending vibrations of PO_4, BO_4, and B−O−P groups.[23]

Crystal Structure. The structure of VBPO-CJ27 consists of a macro-anionic framework $[VB_3P_2O_{12}(OH)]^{2-}$, and the charge neutrality is achieved by Na^+ ions. One asymmetric unit contains one crystallographically unique V site, one unique P site, and three unique B sites (Figure 5a). The V and B atoms locate on the mirror plane. The V atom is octahedrally coordinated to four μ-O atoms shared with adjacent P atoms (V(1)−O(2), 1.998(7) Å; V(1)−O(8), 1.986(6) Å) and one μ_3-O atom bonded to two tetrahedrally coordinated B atoms (V(1)−O(3), 2.262(6) Å), leaving one terminal O atom (V(1)−O(1), 1.575(6) Å). The P atom is in a tetrahedral environment sharing O atoms with two adjacent V atoms (P(1)−O(2), 1.480(6) Å; P(1)−O(8), 1.498(7) Å) and two B atoms (P(1)−O(6), 1.527(6) Å; P(1)−O(7), 1.521(6) Å). Of the three distinct B sites, B(1) and B(2) atoms are tetrahedrally coordinated to three μ-O atoms and one μ_3-O atom (B−O, 1.434(12)−1.481(8) Å). The B(3) atom shares two bridging O atoms with B(1) and B(2) atoms, leaving a terminal hydroxyl group to form a trigonal plane (B−O, 1.344(16)−1.380(16) Å). The selected bond lengths and angles of VBPO-CJ27 are shown in Table 2.

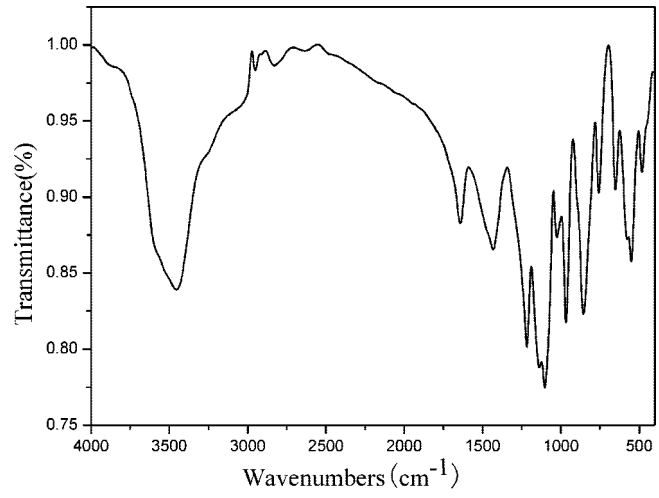

Figure 4. Infrared spectrum of VBPO-CJ27.

The linkage of VO_6 octahedra, PO_4 and BO_4 tetrahedra, and $BO_2(OH)$ trigonal planes leads to the open framework of VBPO-CJ27. It is featured by a structural building cluster containing one VO_6 octahedron, four PO_4 tetrahedra, and one $[B_3O_7(OH)]$ 3-ring motif, which is composed of one $BO_2(OH)$ trigonal plane and two BO_4 tetrahedra (Figure 5b). Such building clusters are connected through sharing PO_4 tetrahedra to form a B−P−V−O 12^816^6 supercavity (Cavity I) as seen in Figure 6. This super cavity is built from the P−V−O 12^816^6 cavity (Cavity II) with pendent $[B_3O_7(OH)]$ 3-ring motifs. On the other hand, Cavity I can also be viewed as the connection of distorted VO_6 octahedra and a B−P−O 12^820^6 supercavity (Cavity III). The super-Cavities I are further connected with each other through sharing the building clusters shown in Figure 5b to form the complex channel system of VBPO-CJ27, which contains parallel 8- and 16-ring channels formed by VO_6 and PO_4 polyhedra along the [100], [010], and [001] directions (Figure 7a), and intersecting 12-ring channels enclosed by BO_4 and PO_4 tetrahedra along the [011], [110], [101], and [111] directions, respectively (Figure 7b). The terminal V−O bonds of VO_6 octahedra and the $[B_3O_7(OH)]$ 3-ring motifs protrude into the 16-ring channels, thus reducing the void space of the framework.

(23) Baykal, A.; Klzilyalli, M. *J. Mater. Sci.* **2000**, *35*, 4621.

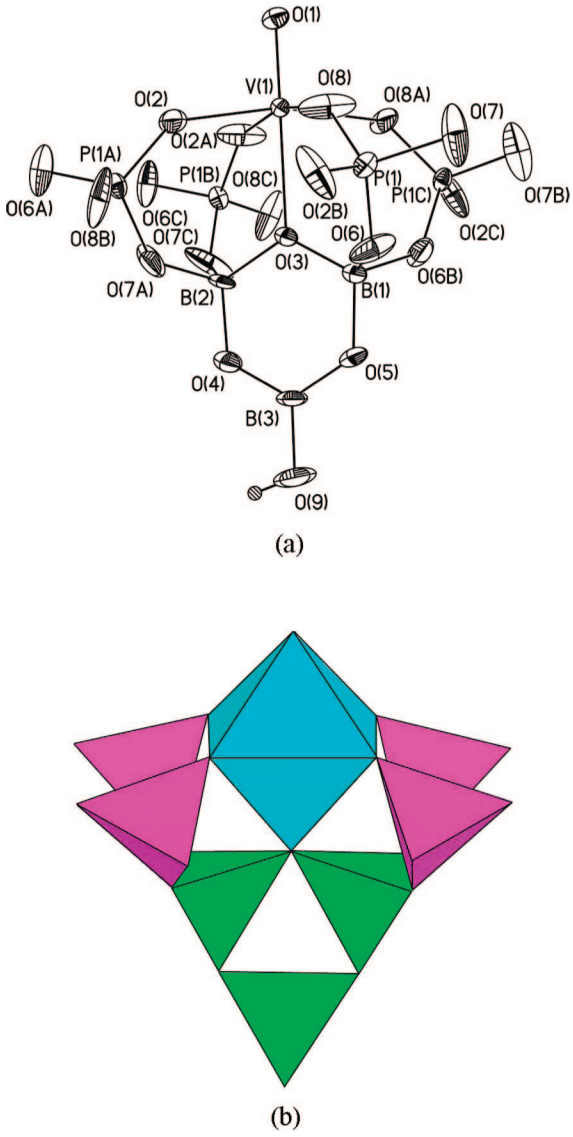

Figure 5. (a) Thermal ellipsoid plots (30% probability) and atomic labeling schemes of the framework in VBPO-CJ27; (b) polyhedral view of the building cluster of VBPO-CJ27. Color code: P, purple; B, green; V, bright blue.

The negative charges of the anionic framework are compensated for by Na^+ ions. Figure 8 shows the coordination environments of the Na^+ ions. The Na^+ ions, which are irregularly coordinated by 6, 8, or 9 oxygen atoms, have weak interactions with the framework. The Na−O distances are listed in Table 2.

As with MBPO-CJ25 (M = Mn, Co, Ni) and its isotype structures,[19] VBPO-CJ27 is one of the few transition-metal borophosphates containing both BO_3 and BO_4 groups with the B/P ratio of 3/2. Insights into the structural characteristics of borophosphates indicate that only a few compounds have 3-D anionic partial structures, all of which contain tetrahedral borates and phosphates with 12- or 8-ring openings.[12,16,17] The 3-D anionic partial structure of VBPO-CJ27 consists of mixed coordinated borates and tetrahedral phosphates and is featured by 16- and 20-ring openings viewed along the crystal axis (Figure 9, right) and 12-ring openings viewed along the diagonal directions (see Figure 7b). The fundamental building unit (FBU) of the anionic partial structure

Table 2. Selected Bond Lengths [Å] and Angles [deg] for VBPO-CJ27[a]

V(1)−O(1)	1.575(6)	O(8)#1−V(1)−O(2)#1	91.7(4)
V(1)−O(8)	1.986(6)	O(2)−V(1)−O(2)#1	87.9(6)
V(1)−O(8)#1	1.986(6)	O(1)−V(1)−O(3)	180.0(4)
V(1)−O(2)	1.998(7)	O(8)−V(1)−O(3)	83.2(2)
V(1)−O(2)#1	1.998(7)	O(8)#1−V(1)−O(3)	83.2(2)
V(1)−O(3)	2.262(6)	O(2)−V(1)−O(3)	83.3(2)
P(1)−O(2)#2	1.480(6)	O(2)#1−V(1)−O(3)	83.3(2)
P(1)−O(8)	1.498(7)	O(2)#2−P(1)−O(8)	113.3(5)
P(1)−O(7)	1.521(6)	O(2)#2−P(1)−O(7)	109.7(4)
P(1)−O(6)	1.527(6)	O(8)−P(1)−O(7)	107.3(6)
B(1)−O(3)	1.437(12)	O(2)#2−P(1)−O(6)	108.7(5)
B(1)−O(5)	1.439(11)	O(8)−P(1)−O(6)	110.5(3)
B(1)−O(6)	1.481(8)	O(7)−P(1)−O(6)	107.2(5)
B(1)−O(6)#1	1.481(8)	O(3)−B(1)−O(5)	116.4(7)
B(2)−O(4)	1.434(12)	O(3)−B(1)−O(6)#1	110.5(5)
B(2)−O(7)	1.463(9)	O(5)−B(1)−O(6)#1	105.1(6)
B(2)−O(7)#3	1.463(9)	O(3)−B(1)−O(6)	110.5(5)
B(2)−O(3)#4	1.474(11)	O(5)−B(1)−O(6)	105.1(6)
B(3)−O(5)	1.380(16)	O(6)#1−B(1)−O(6)	108.9(10)
B(3)−O(9)	1.344(16)	O(4)−B(2)−O(7)#3	106.3(5)
B(3)−O(4)#5	1.380(16)	O(4)−B(2)−O(7)	106.3(5)
O(1)−V(1)−O(8)	96.8(3)	O(7)#3−B(2)−O(7)	107.4(11)
O(1)−V(1)−O(8)#1	96.8(3)	O(4)−B(2)−O(3)#4	116.6(9)
O(8)−V(1)−O(8)#1	85.4(6)	O(7)#3−B(2)−O(3)#4	109.9(5)
O(1)−V(1)−O(2)	96.7(3)	O(7)−B(2)−O(3)#4	109.9(5)
O(8)−V(1)−O(2)	91.7(4)	O(5)−B(3)−O(9)	119.8(12)
O(8)#1−V(1)−O(2)	166.5(2)	O(5)−B(3)−O(4)#5	120.2(9)
O(1)−V(1)−O(2)#1	96.7(3)	O(9)−B(3)−O(4)#5	120.0(12)
O(8)−V(1)−O(2)#1	166.5(2)		
Na(1)−O(2)#2 4×	2.665(10)	Na(3)−O(6)#9 2×	2.529(17)
Na(1)−O(8)#2 4×	2.654(10)	Na(4)−O(1)#6 2×	2.455(9)
Na(2)−O(7)#1 6×	2.948(7)	Na(4)−O(1)#10 2×	2.409(9)
Na(2)−O(4)#7 3×	2.78(2)	Na(4)−O(1W) 2×	3.029(9)
Na(3)−O(2W)	1.97(4)	Na(5)−O(3W)#8 3×	2.91(4)
Na(3)−O(1W)#8	2.66(5)	Na(5)−O(9)#7 3×	2.848(12)
Na(3)−O(5)#7 2×	2.546(9)		

[a] Symmetry transformations used to generate equivalent atoms: #1 x, $-z+1$, $-y+1$; #2 $z-1/2$, $-y+3/2$, $-x+1/2$; #3 $y-1$, $x+1$, z; #4 $-y+1/2$, $z+1/2$, $-x+1/2$; #5 $-z+1/2$, $-x+1/2$, $y-1/2$; #6 $-x$, $-y+1$, z; #7 $y-1$, $-z+1$, $-x$; #8 $-x-1/2$, $-y+3/2$, $z-1/2$; #9 $-z$, $x+1$, $-y+1$; #10 x, $-y+1$, $-z+1$.

in VBPO-CJ27 according to the categories by Kniep et al.[3] is composed of a $[B_3O_7(OH)]$ 3-ring motif and two PO_4 tetrahedra (Figure 9, left). It is the same as that in MBPO-CJ25 (M = Mn, Co, Ni)[19] with a 1-D borophosphate anionic chain. Such a FBU rarely occurs in borophosphate anionic partial structures. It is the first time it has been observed in 3-D anionic partial structure, particularly in the cavity structure.

Among the metal borophosphate compounds, vanadium borophosphates with rich anionic structures, especially the clusters, have been reported.[24–28] Most of the vanadium borophosphate clusters contain several V atoms in each cluster unit. Only $[N_2C_6H_{14}]_2VO(PO_3OH)_4(B_3O_3OH)\cdot 4H_2O$[29] and $(C_6H_{14}N_2)_2[VO(HPO_4)_5B_2O]\cdot H_2O$[30] have anionic structures with a single vanadium center. The building cluster of VBPO-CJ27 shown in Figure 5b is very similar to these two clusters. However, all O atoms of the PO_4 tetrahedra in

(24) Bontchev, R. P.; Do, J.; Jacobson, A. J. *Angew. Chem., Int. Ed.* **1999**, *38*, 1937.
(25) Do, J.; Bontchev, R. P.; Jacobson, A. J. *Inorg. Chem.* **2000**, *39*, 4305.
(26) Do, J.; Bontchev, R. P.; Jacobson, A. J. *Inorg. Chem.* **2000**, *39*, 3320.
(27) Engelhardt, H.; Borrmann, H.; Schnelle, W.; Kniep, R. *Z. Anorg. Allg. Chem.* **2000**, *626*, 1647.
(28) Zhang, L.-R.; Zhang, H.; Borrmann, H.; Kniep, R. *Z. Kristallogr. - New Cryst. Struct.* **2002**, *217*, 477.
(29) Bontchev, R. P.; Do, J.; Jacobson, A. J. *Inorg. Chem.* **1999**, *38*, 2231.
(30) Wikstad, E.; Kritikos, M. *Acta Crystallogr.* **2003**, *C59*, m87.

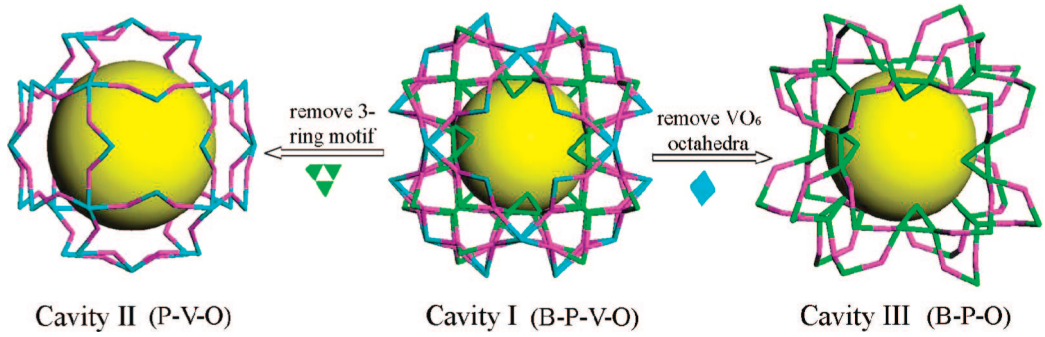

Figure 6. Relationship of Cavities I, II, and III. The O atoms are removed for clarity. Color code: P, purple; B, green; V, bright blue.

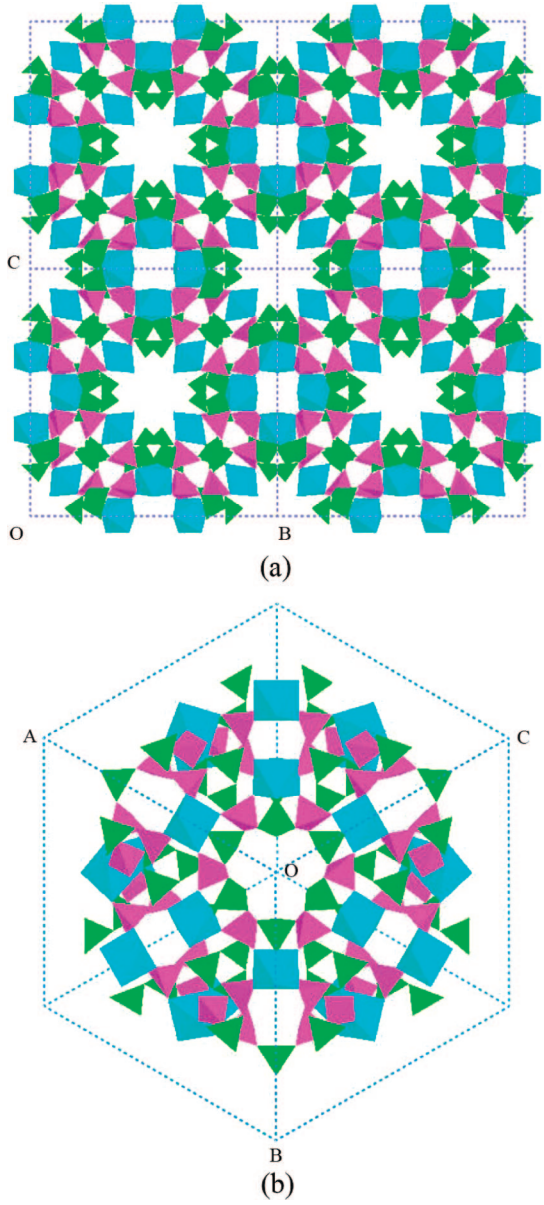

Figure 7. (a) Parallel 8- and 16-ring channels of VBPO-CJ27 viewed along the [100] direction; (b) the 12-ring channels viewed along the [111] direction. Color code: P, purple; B, green; V, bright blue.

VBPO-CJ27 are shared, whereas terminal oxygen atoms exist in the $PO_2O_t(OH)$ (O_t: terminal O atom) tetrahedra in the above-mentioned clusters. The reason might be due to that in the syntheses of $[N_2C_6H_{14}]_2VO(PO_3OH)_4(B_3O_3OH)\cdot 4H_2O$[29] and $(C_6H_{14}N_2)_2[VO(HPO_4)_5B_2O]\cdot H_2O$,[30] organic

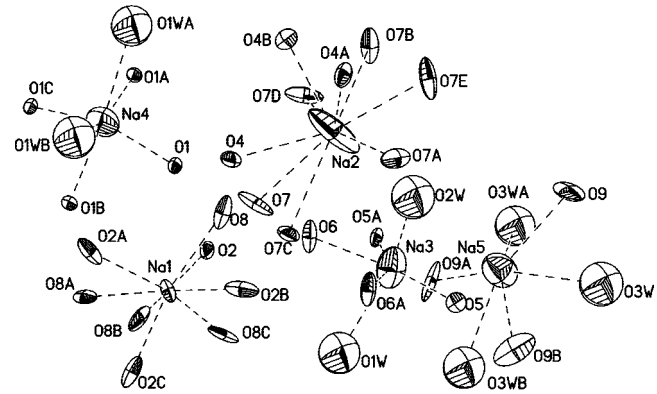

Figure 8. Coordination environments of Na^+ ions in VBPO-CJ27.

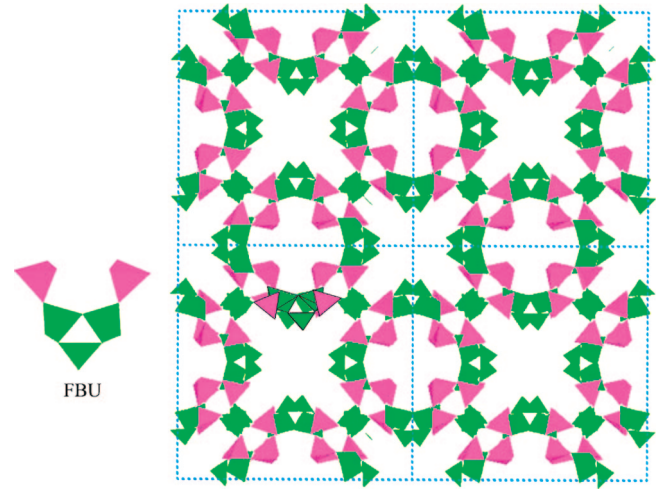

Figure 9. FBU of the anionic partial structure in VBPO-CJ27 (left) and the 3-D borophosphate anionic open framework of VBPO-CJ27 viewed along the [001] direction showing 16- and 20-ring openings (right). Color code: P, purple; B, green; V, bright blue.

molecules were used as the structure-directing agents, which stabilize the terminal P═O and P−OH groups of the clusters through hydrogen bonds and, thus, interrupt the further connection of the clusters. However, for VBPO-CJ27 only inorganic species are involved, and the four-connected PO_4 groups are shared by neighboring building clusters, leading to a 3-D framework.

To the best of our knowledge, VBPO-CJ27 is the first example of open-framework borophosphate containing extra-large 16-ring channels formed by the connection of $12^8 16^6$ supercavities.

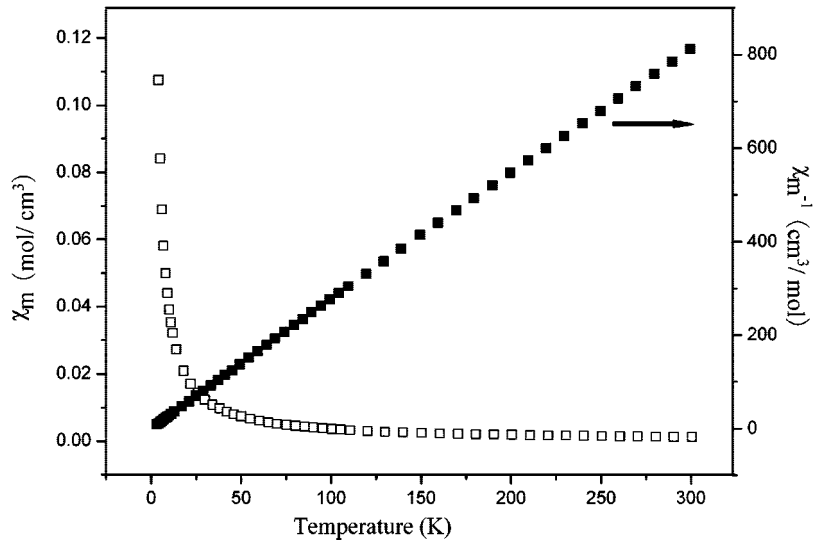

Figure 10. χ_m vs T and $1/\chi_m$ vs T plots of VBPO-CJ27.

Properties. The temperature dependences of the magnetic susceptibilities of VBPO-CJ27 were studied at an applied magnetic field of 5000 Oe over the temperature range of 4−300 K. Figure 10 shows the plots of χ_m and $1/\chi_m$ versus T of the compound. Magnetic measurements confirmed that vanadium is present as V^{4+} as expected from stoichiometry and the bond valence calculation. The compound is a simple paramagnet, and the susceptibility obeys the Curie−Weiss rule with an effective magnetic moment per V^{4+} calculated from the derived Curie constant of 1.73 μ_B. It is consistent with the isolated V^{4+} ion ($3d^1$, $S = 1/2$).

The ion-exchange capacities of VBPO-CJ27 with K^+, Li^+, and NH_4^+ ions have been studied. The result shows that the Na^+ ions in VBPO-CJ27 can be exchanged only by NH_4^+ ions in a melt of $(NH_4)_2HPO_4$ at 200 °C and that the exchange amount is approximately 22%.

Conclusion

A new open-framework vanadium borophosphate VBPO-CJ27 with extra-large 16-ring channels was prepared by employing the boric acid flux method. It is constructed from the connection of single vanadium-centered building clusters comprised of VO_6 octahedra, PO_4 and BO_4 tetrahedra, and $BO_2(OH)$ trigonal planes to form intersecting 8-, 12-, and 16-ring channels. The 3-D anionic partial structure has a B/P ratio of 3/2 and contains 12-, 16-, and 20-ring openings. Notably, VBPO-CJ27 possesses unprecedented $12^8 16^6$ supercavities in the structure. Magnetic measurement reveals that the compound is paramagnetic. Ion-exchange studies show that the Na^+ ions can be partly exchanged by NH_4^+. The successful synthesis of VBPO-CJ27 demonstrates that diverse open-framework borophosphate materials with interesting framework structures might be accessed synthetically by using the boric acid flux method.

Acknowledgment. This work is supported by the National Natural Science Foundation of China, the State Basic Research Projects of China (2006CB806103 and 2007CB936402), and the Major International Joint Research Project of China.

Supporting Information Available: The crystallographic data in CIF format for VBPO-CJ27. This material is available free of charge via the Internet at http://pubs.acs.org.

CM8000283